SWITCHED RELUCTANCE MOTOR DRIVE SYSTEMS DYNAMIC PERFORMANCE PREDICTION AND EXPERIMENTAL VERIFICATION

A.A. Arkadan, Senior Member **B.W. Kielgas, Student Member**

Electrical and Computer Engineering Department
Marquette University
Milwaukee, WI 53233-2286

Abstract: In this first of a set of two companion papers on switched reluctance motor drive systems, the results of using a state space model to predict a motor-drive system dynamic performance characteristics under normal operating conditions are presented. Using this approach, the state space model parameters are determined from series of nonlinear magnetic field solutions, thus accounting for magnetic material nonlinearities and space harmonics due to the motor geometry. The method is applied to a 6/4, 0.15 hp, 5000 r/min switched reluctance motor and resulted in the machine inductances, which compared favorably to measured values. Using these parameters in the state space model, the dynamic performance characteristics of the motor drive system are predicted and verified by comparison to experimental data. In addition, the effects of mutual coupling between motor phases on the analysis results are evaluated.

Keywords: Switched Reluctance Motor Drive Systems
Parameters Determination
Dynamic Performance Prediction

INTRODUCTION

Switched reluctance motors (SRM's) were developed in the late 1800's, but have seen little use in practical applications. They are among the simplest of all rotating machinery. These motors have no form of excitation on the rotor, which eliminates the need for brushes or slip rings, and this type of motor is quite rugged and durable with little need for servicing or upkeep. In spite of these apparent advantages over other types of motors, the SRM's have not been widely used until recently because of the difficulties involved in their control. However, with the advances in control technology and the availability of power electronic components, switched reluctance motors are being developed for a wide variety of applications as an alternative to other types of motors where a high degree of reliability is required. Because of this, much of the recent literature concerning switched reluctance motors has been centered on the development of low cost drive systems and effective methods for controlling the devices [1-5]. In addition, much effort has gone into developing effective ways for modeling switched reluctance motors in order to optimize their design and operation. Singh and Kuo [6] utilized a state model approach with measured incremental inductance values in order to model the performance of an 8/6 switched reluctance motor. Stephenson and Corda [7] used a similar method with the exception that measured flux linkage/current/rotor position data was used to calculate the torque and current of a switched reluctance motor. Manzer et al [8] used a similar approach with a bivariate polynomial representation of the measured flux linkage data. Torrey and Lang [9] presented a model which is based on the use of measured flux linkages/current/rotor position curves to account for magnetic nonlinearities of the motor. The drawback with these approaches is that measured motor parameter data is used, which requires the construction of the actual device. Other approaches involving the use of magnetic field solutions can be found in the literature [10,11]. In the work of Wallace and Taylor [10], magnetic field solutions were used to model an SRM in a study to reduce the torque ripple. Meanwhile, in the work of Moallem et al [11] magnetic field solutions were used to predict the torque of switched reluctance machines utilizing a variety of approaches. In most of the published literature on SRM drives the effects of mutual inductances were neglected when predicting the SRM drive system performance due to the nature of the motor. However, in the work of Moriera and Lipo [12], these effects were studied for a four phase SRM. Also Peterson and Lyons presented a model which accounts for mutual coupling and suitable for SRM drives with multi-phase excitation [13].

In this work, a state space modeling approach is presented which is based on the use of series of nonlinear finite element magnetic filed solutions to determine the self and mutual inductances of a SRM. The main advantage of using this modeling approach, in comparison to other approaches [6-13], is its suitability for integration in an iterative approach to predict the system performance under fault conditions as described in a companion paper [14]. Other advantages include the ability to account for nonlinearities due to material saturation and the effects of space harmonics due to the motor geometry. In this paper, the state space modeling approach is presented. Furthermore, the effects of mutual coupling between motor phases are evaluated and the performance characteristics of the SRM drive system are predicted under normal operating conditions and verified by comparison to measured data.

SWITCHED RELUCTANCE MOTOR DRIVE SYSTEM DESCRIPTION

The Switched Reluctance Motor drive system consists of the SRM itself, the inverter used to supply power to the motor, the controller used to control the switching of the inverter, and the hysteresis brake used to load the motor. A block diagram of the drive system is shown in Figure (1). The SRM utilized for the analysis is a 6/4 machine, where 6 designates the number of stator poles and 4 designates the number of rotor poles. The three-phase motor has a 0.15 hp rating at 5000 r/min. A cross section of the machine is shown in Figure (2). The coils of diametrically opposite stator poles are connected in series to aid each other and to form one phase of the machine. The

93 WM 025-7 EC A paper recommended and approved by the IEEE Electric Machinery Committee of the IEEE Power Engineering Society for presentation at the IEEE/PES 1993 Winter Meeting, Columbus, OH, January 31 - February 5, 1993. Manuscript submitted September 1, 1992; made available for printing December 28, 1992.

motor consists of three phase windings designated as (a), (b), and (c). The inverter configuration used for this analysis is shown in Figure (3). The switching sequence in which each phase is 'on' for 30° is shown in Figure (4). When a phase is 'on', the two transistors for that phase are turned 'on' and the dc supply voltage is placed across the phase winding. When a phase is 'off', the transistors are turned 'off' and the energy stored in the motor winding is returned through the antiparallel diodes to the dc source. This inverter configuration is perhaps the simplest of configurations which provide regeneration capability. However, the main disadvantage is that the configuration requires two transistors per phase which dominate the cost of the inverter. A constant speed controller was developed which used position feedback from an optical encoder to switch the motor phases every 30°. In addition, the offset of the switching from a fixed reference was also controlled. For full details, reference [15] should be consulted.

SWITCHED RELUCTANCE MOTOR DRIVE SYSTEM STATE SPACE MODEL DESCRIPTION

A lumped parameter state space model for the dynamic analysis of SRM's, which is based upon a three winding representation of the motor phases, is presented. The three phase windings are designated by (a), (b), and (c). The differential equations used to model the transient and dynamic performance of electrical machines in general are derived from the interaction among the phase windings. Accordingly, for a j^{th} winding in a system of three magnetically coupled coils, a, b, and c, in a given machine, one can write the following for the terminal voltage of the j^{th} coil [16]:

$$v_j = r_j i_j + (\sum_k [\frac{\partial \lambda_j}{\partial i_k} \frac{di_k}{dt}]) + [\frac{\partial \lambda_j}{\partial \theta} \frac{d\theta}{dt}] \qquad (1)$$

Here j, k =a, b, and c. Also, r_j is the Ohmic resistance of the j^{th} winding, λ_j is the flux linkage of the j^{th} winding, and θ is the rotor position from a fixed reference. The first term on the right hand side of equation (1) represents the Ohmic voltage drop, the second term represents the transformer voltage, and the last term represents the rotational voltage. In addition, the term

$$\frac{\partial \lambda_j}{\partial i_k} = L_{jk}^{inc} \qquad (2)$$

represents the incremental inductance of the jk^{th} winding. The superscript *inc* will be removed for simplicity. The term

$$\frac{d\theta}{dt} = \omega_m \qquad (3)$$

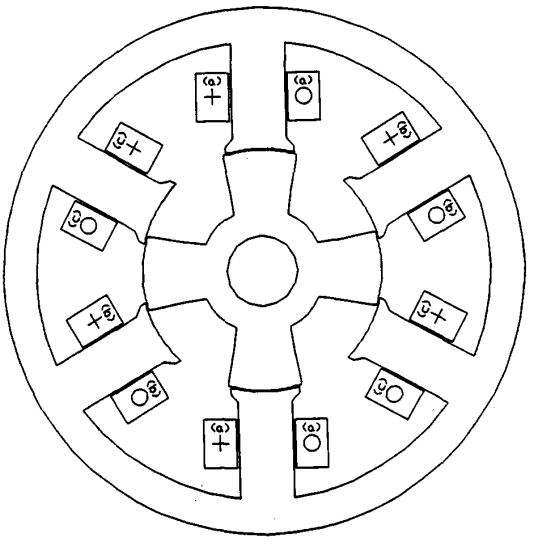

Figure (2): Motor Cross Section

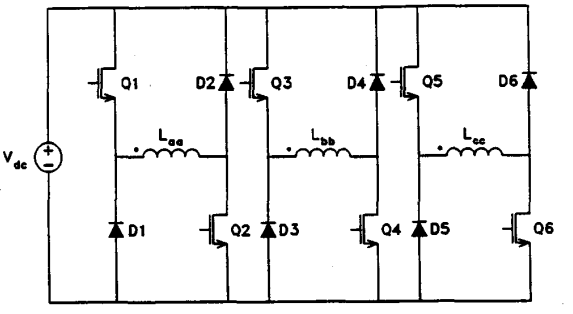

Figure (3): Inverter Configuration

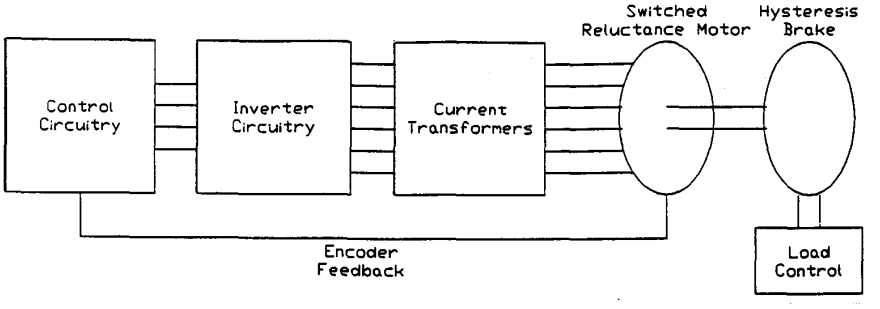

Figure (1): Schematic of the SRM Drive-Load System

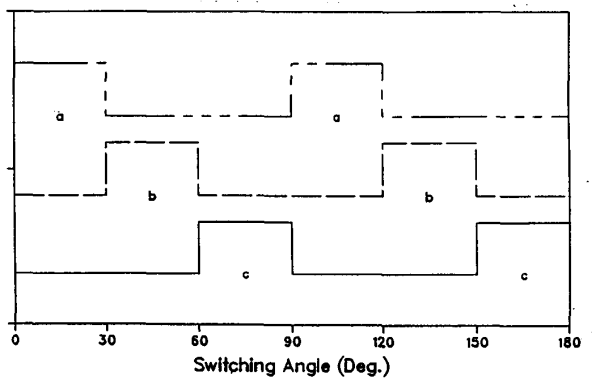

Figure (4): Switching Sequence

represents the mechanical speed in radians per second. Equation (1) can be written in matrix form as:

$$\underline{V} = \underline{R}\,\underline{I} + \underline{L}\frac{d\underline{I}}{dt} + \omega_m \frac{d\underline{L}}{d\theta}\underline{I} \tag{4}$$

where the matrix $\underline{L}$ is:

$$\underline{L} = \begin{bmatrix} L_{aa} & L_{ab} & L_{ac} \\ L_{ba} & L_{bb} & L_{bc} \\ L_{ca} & L_{cb} & L_{cc} \end{bmatrix} \tag{5}$$

As shown in equation (5), the diagonal terms, L_{aa}, L_{bb}, and L_{cc}, represent the SRM self inductances for phases (a), (b), and (c), respectively. Meanwhile, the off diagonal terms, L_{ab}, L_{ba}, L_{ac}, L_{ca}, L_{bc}, and L_{cb}, represent the SRM stator phase to phase mutual inductances. Those mutual inductances are accounted for in the model in order to determine their effects on predicting the device performance. The term $\underline{V}$ in equation (4) is as follows:

$$\underline{V} = \begin{bmatrix} v_a & v_b & v_c \end{bmatrix}^T \tag{6}$$

where v_a, v_b and v_c represent the SRM phase voltages for phases (a), (b) and (c), respectively, and the superscript T denotes the transpose of a matrix. The matrix $\underline{R}$ represents the phase resistances:

$$\underline{R} = \begin{bmatrix} r_a & 0 & 0 \\ 0 & r_b & 0 \\ 0 & 0 & r_c \end{bmatrix} \tag{7}$$

Also the term $\underline{I}$ of equation (4) is as follows:

$$\underline{I} = \begin{bmatrix} i_a & i_b & i_c \end{bmatrix}^T \tag{8}$$

where i_a, i_b, and i_c represent the SRM phase currents.

In addition, the effect of the electromechanical torque on the state model can be determined by incorporating the relationship:

$$\frac{d\omega_m}{dt} = \frac{1}{J}(T_{em} - B\omega_m - T_L) \tag{9}$$

where ω_m is the rotor speed in radians per second, J is the inertia of the rotor, T_{em} is the developed electromechanical torque, B is the coefficient of viscous friction, and T_L is the load torque. The developed torque was calculated using the well known relationship [17]:

$$T_{em} = \frac{P}{\omega_m} \tag{10}$$

where:

$$P = ei \tag{11}$$

and e is the rotational voltage term of equation (4).

The values of the currents i_a, i_b, and i_c, of equation (4), and the rotor speed, ω_m, of equation (9) can be determined numerically for any set of initial conditions and terminal voltages v_a, v_b, and v_c. As can be appreciated from equation (4), the main parameters of the state space model are the stator winding inductances of equation (5). The results of determining these parameters as obtained from nonlinear magnetic field solutions and measurements are discussed below.

STATE SPACE MODEL PARAMETERS DETERMINATION

When considering electronically operated machines, such as the SRM, the currents and mmf's are no longer sinusoidal. In addition, in order to accurately calculate the inductances for the SRM, one must keep in mind that the inductances are dependent on load. Therefore, it is necessary to determine a new set of machine inductances at each load condition. Also, due to the high time rate of change $[di/dt]$ of the currents, accurate knowledge of the self and mutual incremental inductances is necessary when saturation is an important factor, which can be the case with switched reluctance motors.

An energy and current perturbation approach applied to numerical magnetic field solutions provides the basis for the calculation of the machine self and mutual incremental inductances in this work. This approach has been developed and experimentally verified in earlier works [16,18]. In order to calculate the machine self inductances L_{jj} used in the state model equations for the j=a, b, and c windings, the global energy W at the quiescent or operating point is first calculated. Next, the current through the j^{th} coil is perturbed both positively and negatively by a small amount Δi_j where Δi_j is a small amount of the rated current of the machine. This gives two energies, $W(i_j + \Delta i_j)$ and $W(i_j - \Delta i_j)$ which along with the global energy W are used to calculate the incremental self inductance at a given load condition using the following energy expression:

$$L_{jj} = [W(i_j - \Delta i_j) - 2W + W(i_j + \Delta i_j)]/(\Delta i_j)^2 \tag{12}$$

Next, in order to calculate the machine mutual inductances L_{jk} for the j, k = a, b, and c windings, four perturbed energy solutions are required. The current in both the j and k coils is perturbed both positively and negatively by a small amount Δi_j and Δi_k. This gives four energies, $W(i_j + \Delta i_j, i_k + \Delta i_k)$, $W(i_j - \Delta i_j, i_k + \Delta i_k)$, $W(i_j + \Delta i_j, i_k - \Delta i_k)$, and $W(i_j - \Delta i_j, i_k - \Delta i_k)$ which are used to calculate the incremental mutual inductance at a given load condition using the expression:

$$\begin{aligned} L_{jk} = [\ & W(i_j + \Delta i_j, i_k + \Delta i_k) \\ & - W(i_j - \Delta i_j, i_k + \Delta i_k) \\ & - W(i_j + \Delta i_j, i_k - \Delta i_k) \\ & + W(i_j - \Delta i_j, i_k - \Delta i_k)]/(4\Delta i_j \Delta i_k) \end{aligned} \tag{13}$$

Using the above expressions in conjunction with the developed two-dimensional finite element model, the self inductances L_{jj} and the mutual inductances L_{jk} were determined. The calculations were carried out by stepping the rotor in 2° mechanical increments and performing a nonlinear magnetic field solution. The application of this method

resulted in numerical values for the self and mutual inductances versus rotor position. The predicted profile of the stator phase (a) self inductance, L_{aa}, under no load condition is shown in Figure (5) together with the corresponding measured values. Meanwhile, the predicted stator phase to phase mutual inductance, L_{ab}, is shown in Figure (6) together with the corresponding measured values at no load condition. It should be noted that the calculated mutual inductance values are slightly lower in magnitude than the measured inductance values due to the fact that the end windings are not taken into account in the two-dimensional finite element analysis used in this work. The profiles for the self inductances L_{bb} and L_{cc}, are not shown since they are identical to the profile of Figure (5) with the proper phase shift. Also, the profiles for the rest of the mutual inductances are similar to that of Figure (6) except for the phase shift. An inspection of these profiles in Figures (5) and (6) reveals the good agreement between the predicted and measured values of the inductances. Accordingly, it is demonstrated that the computed values of the SRM self and mutual inductances are valid numbers.

Next, in order to use the calculated inductances in the state model of equation (4), the self and mutual inductances were represented by Fourier series type expressions of the form:

$$L_{jk} = c_o + \sum_{n=1}^{NH}[c_n \cos(n\theta - \phi)] \qquad (14)$$

where c_o is the dc value of the inductance, c_n is the magnitude of the n^{th} harmonic, ϕ is the phase shift, and NH is the limit of the harmonic order. The approach was repeated for a load case which resulted in the inductance values. The Fourier series type representation of the inductances at no load and 1.0 per unit (p.u.) load are given in the Appendix.

SYSTEM DYNAMIC PERFORMANCE PREDICTION AND EXPERIMENTAL VERIFICATION

In this section, the results of using the state space model of equations (4) and (9), in conjunction with the computed values of the inductances to predict the dynamic performance of the SRM drive system are presented. It should be emphasized that the effects of space harmonics and magnetic nonlinearities were accounted for in the self and mutual inductances using the approach described above. Furthermore, the results of the inclusion or exclusion of the machine winding mutual inductances on the analysis are presented. In addition, the simulated (predicted) performance characteristics are compared to experimental data for verification. The analysis was performed for two load conditions and the results are given below.

No Load Case:

A steady state analysis was performed using the state space model of equations (4) and (9). The no load self and mutual inductance expressions given in the Appendix were used and the switching sequence shown in Figure (4) was implemented to control the transistors for each phase. Based on this approach, the SRM drive system performance characteristics were determined for the no load steady state operating condition. The predicted current and torque profiles are given by the solid lines in Figures (7) and (8), respectively. In addition, the measured phase (a) current is shown in Figure (9). Furthermore, the

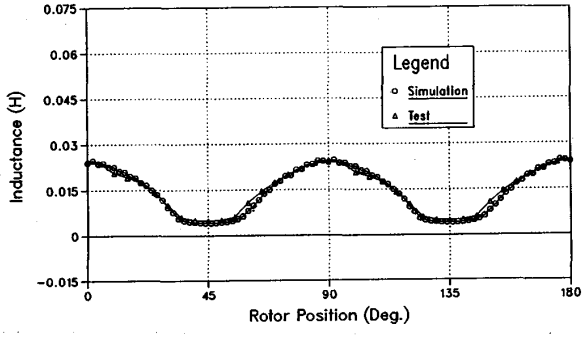

Figure (5): Self Inductance L_{aa}

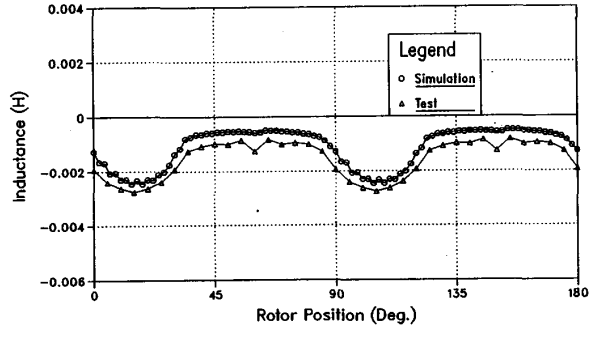

Figure (6): Mutual Inductance L_{ab}

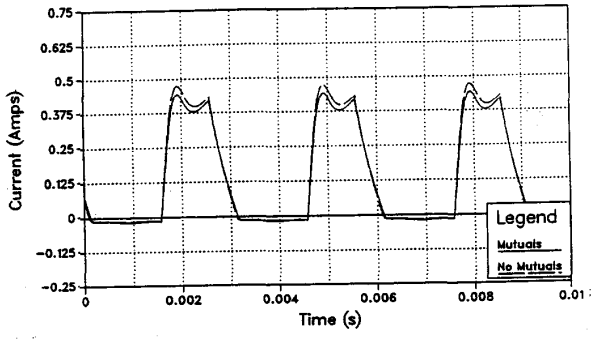

Figure (7): Simulated Phase (a) Current at No Load

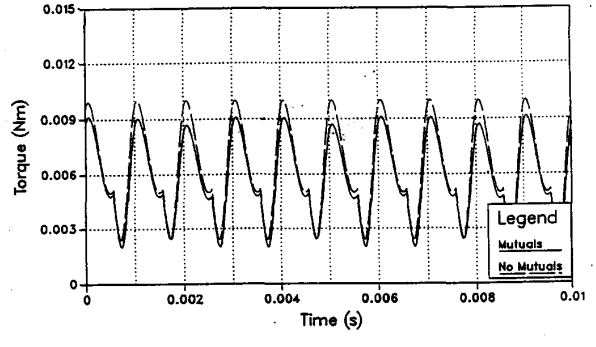

Figure (8): Developed Torque at No Load

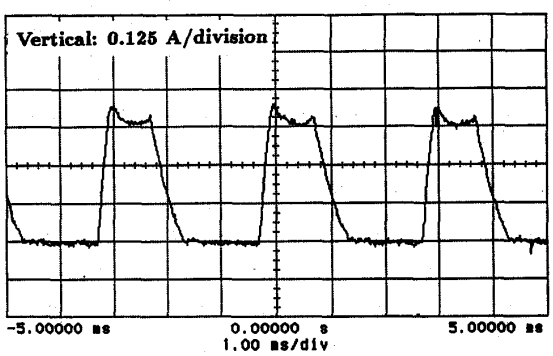

Figure (9): Measured Phase (a) Current at No Load

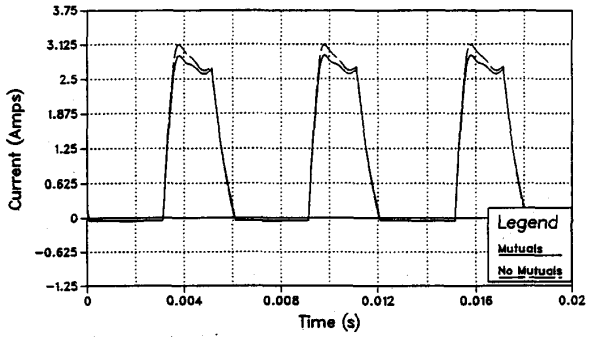

Figure (10): Simulated Phase (a) Current at 1 P.U. Load

values of current, torque, and speed as obtained from simulations and measurements at no load condition are given in Table (1) for comparison purposes.

An inspection of Figures (7) and (9) and the values in Table (1) reveals the good agreement between the simulated and measured results. As can be seen in Table (1), the *dc* component of the stator phase (a) current has a value of 0.150 A as obtained from simulation in comparison to 0.152 A as was found from measurements. In addition, the *rms* value of the phase (a) current was predicted at 0.180 A in comparison to 0.175 A as found from measurements. Finally, the average speed was determined at 523.7 rad/s from simulations while it was measured at 523.6 rad/s. Also, it must be noted that the measured values for the torque used to overcome friction and windage are not available (N/A) for the no load condition.

Next, the effects of neglecting the machine winding mutual inductances, from the state space model, on the SRM dive system predicted performance characteristics, are presented. The analysis was repeated and the mutual inductances were excluded from the state space model. This again resulted in the SRM drive system performance characteristics. The simulated current and torque waveforms are shown by the dashed lines in Figures (7) an (8), respectively. As can be seen from these results, the mutual inductances have a slight effect on the steady state analysis results.

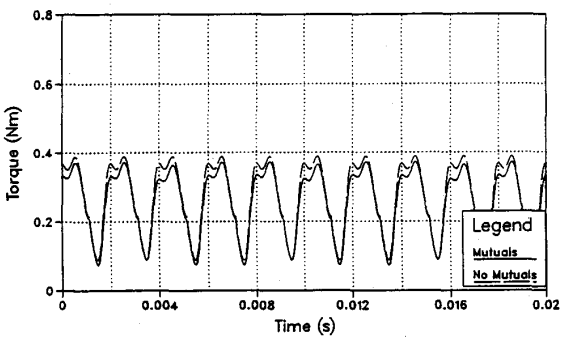

Figure (11): Developed Torque at 1 P.U. Load

1.0 Per Unit Load Case:

Next, a steady state analysis was performed at full load at 2500 r/min. This resulted in the steady state performance characteristic for the SRM drive system. The simulated steady state current and torque profiles are shown by the solid lines in Figures (10) and (11), respectively. In addition, the measured phase (a) current is shown in Figure (12) for this load condition. A comparison of the *dc* and *rms* current, average torque, and average speed values as obtained from simulations and measurements is given in Table (2).

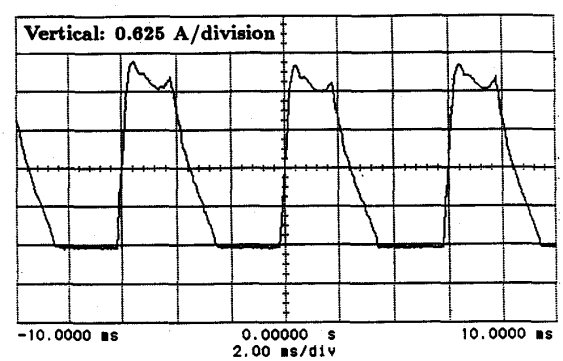

Figure (12): Measured Phase (a) Current at 1 P.U. Load

No Load Operating Condition		
	Simulated	Measured
$I_a(dc)A$	0.150	0.152
$I_a(rms)A$	0.180	0.175
Torque (Avg.) Nm	0.006	N/A
Speed (Avg.) rad/s	523.7	523.6

Table 1: Comparison of Simulated and Test Data at No Load

1 P.U. Load Operating Condition		
	Simulated	Measured
$I_a(dc)A$	0.969	1.080
$I_a(rms)A$	1.220	1.170
Torque (Avg.) Nm	0.253	0.217
Speed (Avg.) rad/s	261.8	261.8

Table 2: Comparison of Simulated and Test Data at 1 P.U. Load

An inspection of Figures (10) and (12) and the numerical values in Table (2) reveals the good agreement between the simulated and measured results. As can be seen in Table (2) the *dc* component of the stator phase (a) current has a value of 0.969 A as obtained from simulation in comparison to 1.08 A as was found from measurements. In addition, the *rms* value of the phase (a) current was found at 1.22 A in comparison to 1.17 A as found from measurements, and the average speed was determined to be 261.8 rad/s from simulations while it was also measured to be 261.8 rad/s. Finally, the computed average value of the developed torque was found at 0.253 Nm and was measured at 0.217 Nm. The discrepancy between the simulated and measured torque values in Table (2) can be attributed to the fact that the measured value for the torque reflects the value of the applied load (hysteresis brake) only. In other words, the measured value in Table (2) represents the applied load torque and does not include the torque needed to overcome friction and windage in the SRM, while the computed value accounts for both.

Again, in order to study the effects of the machine winding mutual inductances on the model, the analysis was repeated neglecting the mutual inductances from the state space model. This resulted in the SRM drive system performance characteristics. The simulated current and torque waveforms for this case are shown by the dashed lines in Figures (10) and (11), respectively. Similar to the no load case, it can be stated that the mutual inductances have a slight effect on the steady state analysis results. This can be explained by noting that the magnetic coupling between the stator phases is usually minimal in this class of machines. In addition, in the case of the SRM drive system considered in this work, only one phase of the SRM is 'on' at any one time, see Figure (4), and relatively low current levels flow in the phase during the regeneration period following the instant a phase is turned off. The effects of accounting for mutual inductances in the analysis model on the simulation results are further examined in a companion paper [14]. In the companion paper, the modeling approach presented here is extended to study the SRM drive system performance under internal and external fault conditions. In such cases, the SRM self and mutual inductance values are updated during the fault condition using an iterative approach. Furthermore, the simulation results are compared to experimental data for verification.

CONCLUSION

A computer aided method for the prediction of the dynamic performance characteristics of switched reluctance motor drive systems under normal operating conditions was presented. The method is general in nature and is based on the use of state space models, in the time domain. The machine parameters were determined from series of nonlinear magnetic field solutions. Accordingly, the effects of material nonlinearities and space harmonics were accounted for in the developed models. This modeling approach was applied to a 6/4, 0.15 hp, 5000 r/min switched reluctance motor and resulted in the machine inductances which compared favorably to measured data. Furthermore, the SRM drive system dynamic performance was predicted at no load and load cases under normal operating conditions and verified by comparison to measured values. In addition, the effects of mutual coupling between motor phases were evaluated and it was demonstrated that the exclusion of the mutual inductances have a slight effect on the analysis results under normal operating conditions for this class of machines.

Appendix

The Fourier expression coefficients at no load condition are given as follows:

Inductance L_{aa}		
DC Value		0.1446E-01
Harmonic	Magnitude	Offset ϕ
4	$0.1066E-01$	$0.2754E+01$
8	$0.5979E-03$	$0.1310E+02$
12	$0.4381E-03$	$0.3206E+02$
16	$0.6090E-03$	$0.1154E+02$
20	$0.1859E-03$	$0.1905E+02$
24	$0.9919E-04$	$0.7650E+02$

Table A.1: Fourier Series Coefficients for L_{aa} at No Load Condition

Inductance L_{ab}		
DC Value		-0.1129E-02
Harmonic	Magnitude	Offset ϕ
4	$0.9168E-03$	$0.6168E+02$
8	$0.3954E-03$	$-0.5540E+02$
12	$0.5812E-04$	$0.3727E+02$
16	$0.5810E-04$	$0.5606E+02$
20	$0.5390E-04$	$-0.5203E+02$
24	$0.1441E-04$	$-0.5424E+02$

Table A.2: Fourier Series Coefficients for L_{ab} at No Load Condition

The Fourier expression coefficients at 1.0 p.u. load condition are given as follows:

Inductance L_{aa}		
DC Value		0.1431E-01
Harmonic	Magnitude	Offset ϕ
4	$0.1068E-01$	$0.4272E+01$
8	$0.3517E-03$	$0.2084E+02$
12	$0.5599E-03$	$0.5148E+02$
16	$0.4487E-03$	$0.1744E+02$
20	$0.1866E-03$	$-0.2523E+02$
24	$0.1429E-03$	$-0.6382E+02$
28	$0.3222E-04$	$0.2141E+02$
32	$0.1237E-03$	$-0.1178E+02$

Table A.3: Fourier Series Coefficients for L_{aa} at 1.0 P.U. Load Condition

Inductance L_{ab}		
DC Value		-0.1100E-02
Harmonic	Magnitude	Offset ϕ
4	$0.8828E-03$	$0.6398E+02$
8	$0.3719E-03$	$-0.4931E+02$
12	$0.9610E-04$	$0.4999E+02$
16	$0.3603E-04$	$0.4488E+02$
20	$0.3892E-04$	$-0.3899E+02$
24	$0.2651E-04$	$-0.3832E+02$
28	$0.8049E-05$	$-0.8396E+01$
32	$0.1218E-04$	$-0.5716E+02$

Table A.4: Fourier Series Coefficients for L_{ab} at 1.0 P.U. Load Condition

References

[1] Davis, R.M., Ray, W.F., and Blake, R.J., "Inverter Drive for Switched Reluctance Motor: Circuits and Component Ratings," *IEE Proceedings*, vol. 128, Pt. B, No. 2, pp. 126-136, March 1981.

[2] Le-Huy, H., Viarouge, P., and Francoeur, B., "Unipolar Converters for Switched Reluctance Motors," *Conference Record of the IAS Annual Meeting pt 1*, pp. 551-560, 1989.

[3] Le-Huy, H., Viarouge, P., and Francoeur, B., "A Novel Unipolar Converter for Switched Reluctance Motor," *IEEE Transactions on Power Electronics*, vol. 5, No. 4, pp. 469-475, October 1990.

[4] Krishnan, R., and Materu, P., "Analysis and Design of a Low Cost Converter for Switched Reluctance Motor Drives," *Conference Record of the IAS Annual Meeting pt 1*, pp. 561-567, 1989.

[5] Krishnan, R. and Materu, P.N., "Design of a Single-Switch-per-Phase Converter for Switched Reluctance Motor Drives," *IEEE Transactions on Industrial Electronics*, vol. 37, No. 6, pp 469-476, December 1990.

[6] Singh, G. and Kuo, B.C., "Modeling and Simulation of Variable- Reluctance Step Motors with Application to a High-Performance Printer System," *IEEE Transactions on Industrial Applications*, vol. 11, No. 4, pp. 373-383, July/August 1975.

[7] Stephenson, J.M. and Corda, J., "Computation of Torque and Current in Doubly Salient Reluctance Motors from Nonlinear Magnetization Data," *IEE Proceedings*, vol. 126, No. 5, pp. 393-396, May 1979.

[8] Manzer, D.G., Varghese, M.W., and Thorp, J.S., "Variable Reluctance Motor Characterization," *IEEE Transactions on Industrial Electronics*, vol. 36, No. 1, pp. 56-63, Feb. 1989.

[9] Torrey, D.A., and Lang, J.H., "Modelling a Nonlinear Variable-Reluctance Motor Drive," *IEE Proceedings*, vol. 137, pp. 314-326, September 1990.

[10] Wallace, R.S., and Taylor, D.G., "Three-Phase Switched Reluctance Motor Design to Reduce Torque Ripple," *ICEM Proceedings*, part 3, pp. 783-787, August 1990.

[11] Moallem, M., and Ong, C.M., "Predicting the Torque of a Switched Reluctance Machine from its Finite Element Field Solution," *IEEE Transactions on Energy Conversion*, vol. 5, No. 4, pp. 733-739, December 1990.

[12] Moreira, J.C., and Lipo, T.A., "Simulation of a Four Phase Switched-Reluctance Motor Including the Effects of Mutual Coupling," *Electric Machines and Power Systems*, Hemisphere, pp. 281-299, 1989.

[13] Preston, M.A. and Lyons, J.P., "A Switched Reluctance Motor Model with Mutual Coupling and Multi-Phase Excitation," *IEEE Transactions on Magnetics*, vol. 27, no. 6, pp. 5423-5425, November 1991.

[14] Arkadan, A.A., and Kielgas, B.W., "Switched Reluctance Motor Drive Systems Dynamic Performance Prediction Under Internal and External Fault Conditions," A companion Paper Submitted for Presentation at the 1993 IEEE-PES, Winter Meeting, Columbus, Ohio.

[15] Kielgas, B.W., "Computer-Aided Analysis of Fault Tolerant Switched Reluctance Motor Drive Systems," Master's Thesis, Marquette University, August 1992.

[16] Arkadan, A.A., Demerdash, N.A., Vaidya, J.G., and Shah, M.J., "Impact of Load Winding Inductances of Permanent Magnet Generators with Multiple Damping Circuits Using Energy Perturbation," *IEEE Transactions on Energy Conversion*, vol. 3, No. 4, pp. 880-889, December 1988.

[17] Fitzgerald, A.E., Kingsley, C., and Umans, S.D., *Electric Machinery*, 4th Edition, McGraw Hill Book Company, 1983.

[18] Nehl, T.W., Fouad, F.A., and Demerdash, N.A., "Determination of Saturated Values of Rotating Machinery Incremental and Apparent Inductances by an Energy Perturbation Method," *IEEE Transactions on Power Apparatus and Systems*, PAS-101, pp. 4441-4451, 1982.

Abdul-Rahman A. Arkadan (S-79, M-88, SM-91) received his B.S. degree from the University of Mississippi in 1980, his M.S. degree from Virginia Polytechnic Institute in 1981, and his Ph.D. degree from Clarkson University in 1988, all in electrical engineering. During the period 1981-1984 he worked in industry. In 1988, he joined the Department of Electrical and Computer Engineering at Marquette University as an Assistant Professor. His interests include design, analysis, and development of electronically-operated machine systems and drives, and computer-aided solution of electromagnetic field problems in electromagnetic devices. He is a member of ASEE, Sigma XI, Phi Kappa Phi, Pi Mu Epsilon, Eta Kappa Nu, Tau Beta PI, and a Registered Professional Engineer in the State of Wisconsin. Dr. Arkadan is a senior member of the IEEE and a member of the IEEE-PES Electric Machinery Committee (EMC) and the IEEE-PES Education Committee. He is the Secretary for the IEEE-PES-EMC Direct Current, Permanent Magnet and Special Machines Subcommittee and a member in several of IEEE-PES subcommittees and working groups.

Bruce W. Kielgas (S-92) received his B.S. degree in electrical engineering from Marquette University in 1990. Also he received his M.S. degree in electrical engineering from Marquette University in August 1992 where he was working in the development of computer models to predict the dynamic performance characteristics of SRM drive systems under normal and fault conditions. Currently Mr. Kielgas is at Westinghouse Electric Corporation at Orlando Florida. His interests include finite element analysis of electromagnetic devices and the computer- aided simulation of power electronic systems. He is a member of IEEE and Tau Beta Pi.

Discussion

Nabeel A. O. Demerdash, Clarkson University, Potsdam, New York: The authors are to be commended on a thorough and complete paper on the modeling of switched reluctance motor drives. Would the authors explain the reasons as to why a choice was made to resort to the currents as the state variables, and consequently the incremental inductances as the machine parameters? rather than the flux linkages as the state variables, and consequently the apparent inductances as the machine parameters [1, 2]. This latter method and formulation has been shown to be quite effective in simulating machine systems with substantial degrees of magnetic circuit saturation. Also, would the authors shed some light on typical flux densities under load and no-load? Perhaps the authors can show some typical flux plots including flux density magnitudes under the simulated conditions.

References

[1] Wang, R., and Demerdash, N. A., "Extra High Speed Modified Lundell Alternator Parameters and Open/Short-Circuit Characteristics from Global 3D-FE Magnetic Field Solutions," *IEEE Transactions on Energy Conversion*, Vol. 7, No. 2, 1992, pp. 330–341.

[2] Demerdash, N. A., and Baldassari, P., "A Combined Finite Element-State Space Modeling Environment for Induction Motors in the ABC Frame of Reference," *IEEE Transactions on Energy Conversion*, Vol. 7, No. 4, 1992, pp. 698–709.

Manuscript received February 22, 1993.

A.A. Arkadan and B.W. Kielgas: These authors wish to express their thanks to Dr. Demerdash for his useful comments and interesting questions included in his discussion. In response to his question on why currents rather than flux linkages were used as state variables, the authors offer the following. In general, for a machine system of n windings, the machine windings terminal voltages and currents are related to the Ohmic resistances and flux linkages as follows:

$$\underline{V} = \underline{R}\underline{I} + \frac{d}{dt}\underline{\Lambda} \tag{1}$$

Moreover, the flux linkages are usually related to the winding currents in two ways. The first is based on using apparent inductances and the second is based on the use of incremental inductances. Using the apparent inductances with equation (1) results in a state space model with flux linkages as state variables:

$$\frac{d}{dt}\underline{\Lambda} = -\underline{R}(\underline{L}^{app})^{-1}\underline{\Lambda} + \underline{V} \tag{2}$$

Meanwhile, using the incremental inductances results in a state space model with currents as state variable:

$$\frac{d}{dt}\underline{I} = -(\underline{L}^{inc})^{-1}\underline{R}\underline{I} + (\underline{L}^{inc})^{-1}(\underline{V} - \underline{E}) \tag{3}$$

As can be noted from both state space models given by equations (2) and (3), the coupling of the motor model to the external circuit model is done by expressing the winding voltages $\underline{V}$ in terms of the external circuit parameters. This can be easily done when currents are used as state variables. In such case, the windings terminal voltages are expressed function of the external circuit currents. Meanwhile, if one opts to use flux linkages as state variables, one needs to express the external circuit equations in terms of flux linkages. This can be easily performed when the external circuits do not include switching electronics as in the case of systems given in references [1,2] of Dr. Demerdash's discussion. However, when the external circuits include switching electronics, as in our case, a disadvantage for using flux linkages as state variables is that certain circuit analysis techniques such as those discussed in references [1] and [2] below have to be modified. In addition, it should be emphasized that the use of currents as state variables and consequently the incremental inductances as parameters was verified to be effective in simulating machines with high degrees of magnetic circuit saturation as was demonstrated earlier [3]. As in the case of the SRM under consideration, the flux plots at no-load and load conditions are given in Figures (1) and (2), respectively. It should be noted that the same magnetic vector potential increments were used in determining the lines of equal potentials (flux contours) for both load conditions. An inspection of both figures reveals the effects of loading and saturation. These effects are clearly evident in Figure (2) as can be seen by the flux leakage contours.

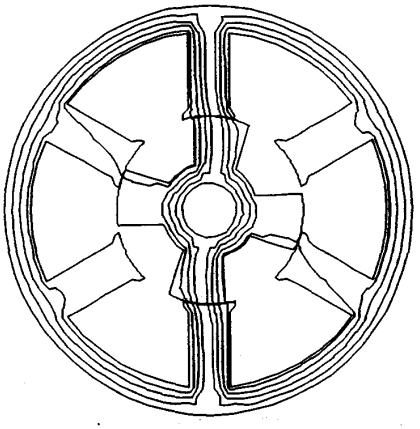

Figure(1): Machine Cross-Section Flux Plot at No-Load

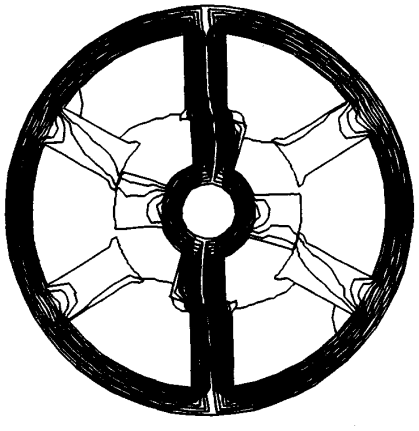

Figure(2): Machine Cross-Section Flux Plot at 1.0 P.U. Load

References

[1] Arkadan, A.A., Hijazi, T.M., Demerdash, N.A., Vaidya, J.G., and Maddali, V.K., "Theoretical Development and Experimental Verification of a DC-AC Electronically Rectified Load-Generator System Model Compatible with common Network Analysis Software Packages", *IEEE Transactions on Energy Conversion*, Vol. EC-3, No. 1, 1988, pp. 123-131.

[2] Chua, L.O., and Lin, P., *Computer-Aided Analysis of Electrical Circuits: Algorithms and Computational Technique*, New Jersey: Prentice-Hall, Inc. 1975.

[3] Arkadan, A.A., Vyas, R., "Effect of Toothless Stator Design on Dynamic Model Parameters of Permanent Magnet Generators", Paper No. 92 SM 570-2 EC presented at the IEEE-PES 1992 Summer Meeting, Seattle, WA, and accepted for publication in the *IEEE Transactions on Energy Conversion*.

Manuscript received April 8, 1993.